ACS APPLIED MATERIALS & INTERFACES

Research Article

www.acsami.org

Thiadiazolo[3,4-*c*]pyridine as an Acceptor toward Fast-Switching Green Donor–Acceptor-Type Electrochromic Polymer with Low Bandgap

Shouli Ming, Shijie Zhen, Kaiwen Lin, Li Zhao, Jingkun Xu,* and Baoyang Lu*

Jiangxi Key Laboratory of Organic Chemistry, Jiangxi Science and Technology Normal University, Nanchang, Jiangxi 330013, China

Supporting Information

ABSTRACT: Thiadiazolo[3,4-*c*]pyridine (PT), an important analog of benzothiadiazole (BT), has most recently been explored as a novel electron acceptor. It exhibits more electron-accepting ability and other unique properties and potential advantages over BT, thus inspiring us to investigate PT-based donor–acceptor-type (D–A) conjugated polymer in electrochromics. Herein, PT was employed for the rational design of novel donor–acceptor-type systems to yield a neutral green electrochromic polymer poly(4,7-di(2,3-dihydrothieno[3,4-*b*][1,4]dioxin-5-yl)-[1,2,5] thiadiazolo[3,4-*c*]pyridine) (PEPTE). PEPTE revealed a lower bandgap ($E_{g,ele}$ = 0.85 eV, $E_{g,opt}$ = 1.12 eV) than its BT analog and also favorable redox activity and stability. Furthermore, electrochromic kinetic studies demonstrated that PEPTE displayed higher coloration efficiency than BT analog, good optical memory, and very fast switching time (0.3 s at all three wavelengths), indicating that PT would probably be a promising choice for developing novel neutral green electrochromic polymers by matching with various donor units.

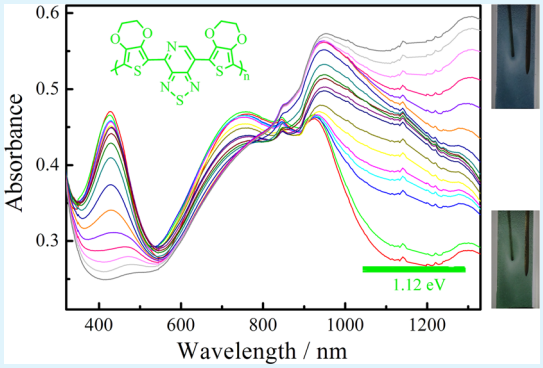

KEYWORDS: *donor–acceptor-type conjugated polymers, green electrochromics, PEDOT, thiadiazolo[3,4-c]pyridine, low bandgap*

1. INTRODUCTION

Combining high contrast ratio, superior coloration efficiency, and multicolor, conjugated polymers have been developed to be the most attractive electrochromic materials.[1−6] Toward electrochromic polymers with specific colors, numerous approaches have been employed to control the color of the polymer, including increasing the conjugation length, utilizing donor–acceptor effect, modifying the HOMO–LUMO levels, and using sterically hindered substituent.[7−12] Also, side chain substituents provide a viable method to tune optical properties of the polymer.[12]

Recently, the Reynolds group started to explore sterically hindered "classical" PEDOT derivatives for colorful electrochromic polymers.[11] However, the approach failed to achieve the green leg of RGB (red–green–blue) color space, which is due to green electrochromic polymers showing dual-band absorption located in the red and blue areas of visible spectrum, respectively, and the absorption could decrease in the oxidized process. Of all the approaches, the donor–acceptor method was the most available for green electrochromic polymers, which has been proven by the breakthrough discovery by Wudl and co-workers.[13,14] Soon after this pioneering work, dozens of green electrochromic polymers containing alternating different donors and benzothiadiazole analogs/derivatives have been achieved (their structures are shown in Scheme 1),[15−27] some of which display relatively low bandgap, fast switching time, and exceptional long-term stability (Table S1, Supporting Information). Despite these efforts devoted to green polymeric electrochromics, the fundamental research and applications are far from prosperity and still have significant scope for development.

The most common and effective strategy toward green electrochromic polymers consists of tailoring the nature and structural control of donors and acceptors in the donor–acceptor-type (D–A) polymers. It has clearly been demonstrated that compositions not only change the redox potentials and bandgap of these polymers but also modify the electrochromic performances including switching color, optical contrast, color efficiency, and stability.[1−5] For D–A polymers, bandgap (E_g) reduction has been demonstrated to be an effective way to achieve optical contrast and stable electrochromic polymers.[4,8,9] Previous studies proved that bandgaps of D–A conjugated polymers primarily depend on the acceptor moiety.[19,28,29] Therefore, inserting an electron-deficient acceptor into the π-conjugated system probably develops a decreased bandgap material.

Because of the π-electron deficient nature of pyridine unit compared to benzene, pyridine (PT) would be a stronger acceptor unit relative to benzothiadiazole (BT).[30−32] In the donor–acceptor-type neutral green electrochromic polymer

Received: October 19, 2014
Accepted: May 8, 2015
Published: May 8, 2015

DOI: 10.1021/acsami.5b01188
ACS Appl. Mater. Interfaces 2015, 7, 11089−11098

Scheme 1. Chemical Structures of Donor−Acceptor-Type Neutral Green Electrochromic Polymers Reported Previously[15−27]

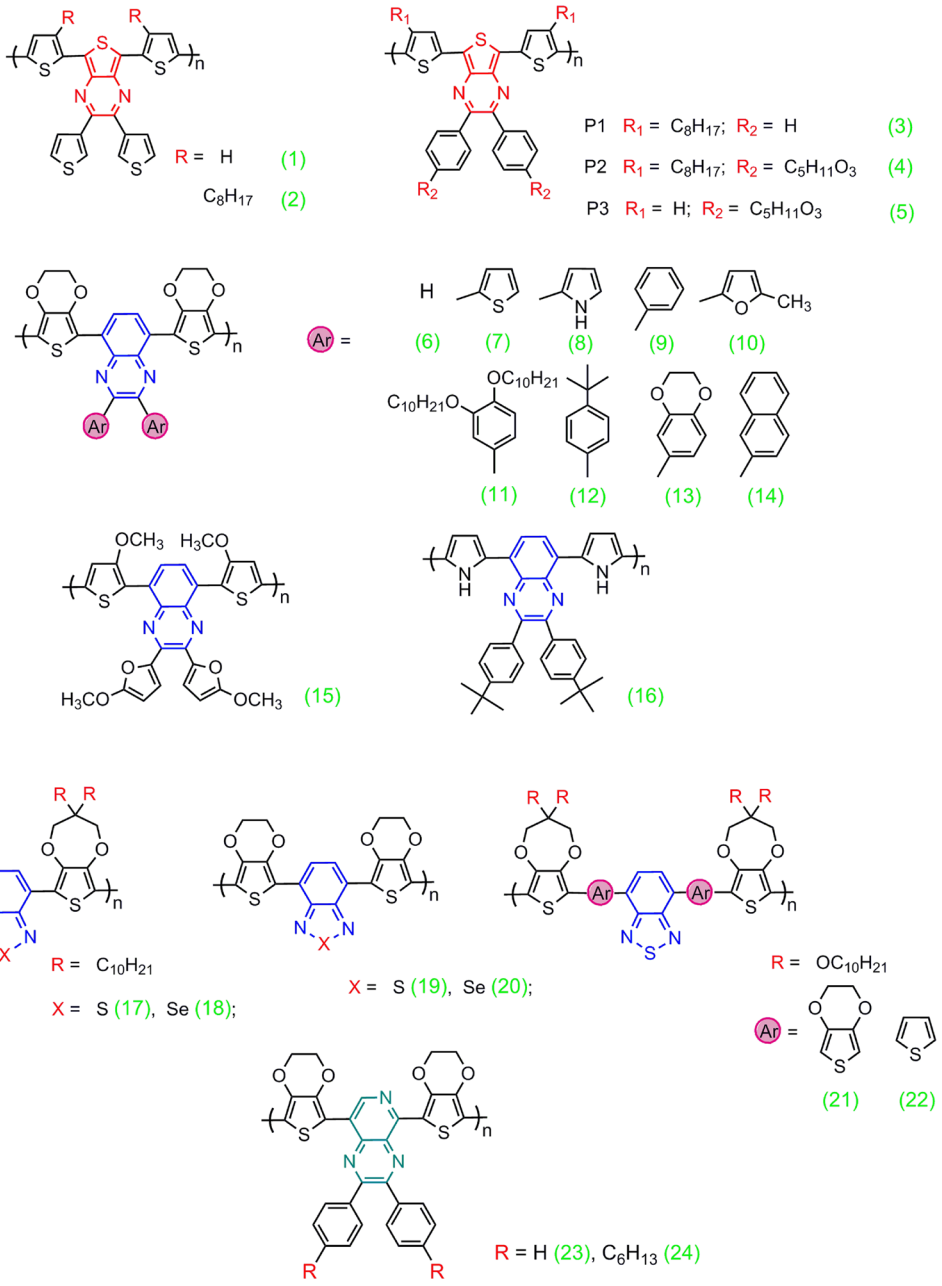

family, in sharp contrast to benzothiadiazole derivatives and thieno[3,4-*b*]pyrazine derivatives extensively employed as acceptor units, PT has scarcely been explored (Scheme 1).[13−27,32−35] Recently, Zhou et al.[29] incorporated thiadiazolo-[3,4-*c*]pyridine derivative with weak donor units to yield a series of polymers showing better solubility, lower bandgap, and deeper HOMO and LUMO levels compared to BT-based polymers, which stimulated us to investigate electrochromic performances of the polymers containing PT constructed using the donor−acceptor strategy.

Recently, we developed several typical 3,4-ethylenedioxythiophene (EDOT)-based copolymers as promising electrochromic materials, such as furan-EDOT, selenophene-EDOT, and PEDOT network films.[37−40] Considering the unique electrochromic performances of EDOT-based copolymers, EDOT was herein employed as the donor unit toward the construction of the novel D−A system, 4,7-di(2,3-dihydrothieno[3,4-*b*][1,4]dioxin-5-yl)-[1,2,5]thiadiazolo[3,4-*c*]pyridine (EPTE). The optical properties, intramolecular charge transfer properties, density functional theory calculations, and electrochemical polymerization of the precursor were reported. Furthermore, the structure and morphology, electrochemistry, spectroelectrochemistry, and electrochromic performances of the electrosynthesized neutral green polymer were explored in detail. Herein, the resulting conducting polymer containing PT was discussed in comparison with its close analog, 4,7-di(2,3-dihydrothieno[3,4-*b*][1,4]dioxin-5-yl)-benzo[1,2,5]thiadiazole (EBTE).

2. EXPERIMENTAL METHODS

Materials. 3,4-Ethylenedioxythiophene (EDOT, 98%; Sigma-Aldrich), 2,3-diaminopyridine (98%; Shanghai Vita Chemical Reagent Co., Ltd.), thionyl bromide ($SOBr_2$, 97%; J&K Scientific Ltd.), bromine (Br_2, 98%; J&K Scientific Ltd.), hydrobromic acid (HBr,

DOI: 10.1021/acsami.5b01188
ACS Appl. Mater. Interfaces 2015, 7, 11089−11098

48%; J&K Scientific Ltd.), *n*-butyllithium (*n*-BuLi, 2.5 mol L^{-1} in hexanes; Energy Chemical), chlorotributyltin ($SnBu_3Cl$, Energy Chemical), tetrakis(triphenylphosphine)palladium (0) ($Pd(PPh_3)_4$, 99%; Energy Chemical), and acetonitrile (MeCN, 99.9%; Xilong Chemical) were used directly without further purification. Lithium perchlorate ($LiClO_4$, 98%; Energy Chemical), tetrabutylammonium hexafluorophosphate (Bu_4NPF_6, 98%; Energy Chemical), and tetrabutylammonium tetrafluoroborate (Bu_4NBF_4, 98%; Energy Chemical) were dried under vacuum at 60 °C for 24 h before use. Tetrahydrofuran (THF, analytical grade; Xilong Chemical), dimethylformamide (DMF, analytical grade; Xilong Chemical), and dichloromethane (CH_2Cl_2, analytical grade; Shanghai Vita Chemical Reagent Co., Ltd.) were purified by distillation with calcium hydride under a nitrogen atmosphere.

Characterizations. ^1H NMR and ^{13}C NMR spectra were measured by using a Bruker AV 400 NMR spectrometer. With a SPECORD PLUS UV−vis spectrophotometer (ANALYTIKJENA, Germany), UV−vis spectra were recorded. Emission spectra of the monomers were determined by using an F-4500 fluorescence spectrophotometer (Hitachi). Scanning electron microscopy (SEM) images were recorded on a VEGA II-LSU scanning electron microscope (Tescan).

Monomer Synthesis. 4,7-Di(2,3-dihydrothieno[3,4-*b*][1,4]dioxin-5-yl)-[1,2,5] thiadiazolo[3,4-*c*]pyridine (EPTE) was synthesized as described in Scheme 2. Compounds II and IV were prepared according to literature procedures.[30,32,41]

Scheme 2. Synthetic Route and Electropolymerization of EPTE

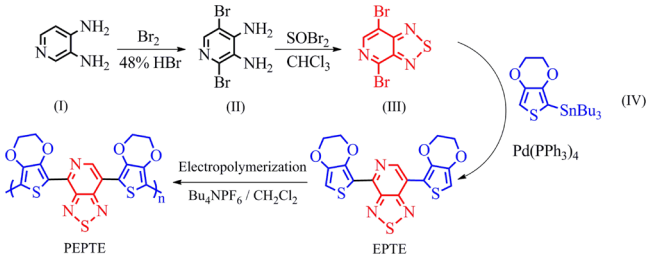

4,7-Dibromo[1,2,5]thiadiazolo[3,4-c]pyridine (III). Under nitrogen atmosphere, a solution of 2,5-dibromo-3,4-diaminopyridine (1.00 g, 3.74 mmol) in anhydrous chloroform (10 mL) was cooled to −0 °C. Then, thionyl bromide (2.25 g, 18.9 mmol) was added dropwise, followed by stirring of the mixture for 30 min. The reaction was stirred at room temperature for 30 min and refluxed at 75 °C. After 8 h of heating, thionyl bromide (2.25 g, 18.9 mmol) was added dropwise again, and the mixture was refluxed for 4 h. The reaction mixture was allowed to cool to room temperature and poured into ice-water. The mixture was neutralized (pH = 8) with solid Na_2CO_3, extracted with ethyl acetate (3 × 10 mL), and dried with anhydrous $MgSO_4$. The solvent was removed by rotary evaporation, and the product was purified by silica column chromatography to obtain 0.57 g of yellow solid (Yield: 52%). ^1H NMR (400 MHz, $CDCl_3$, ppm): δ 8.55 (s, 1H); ^{13}C NMR (400 MHz, DMSO-d_6, ppm): δ 155.24, 150.26, 145.24, 136.66, 111.69.

4,7-Di(2,3-dihydrothieno[3,4-b][1,4]dioxin-5-yl)-[1,2,5]-thiadiazolo[3,4-c]pyridine (EPTE). To a nitrogen-degassed solution of 2-tributylstannyl-3,4-ethylenedioxythiophene (5.84 g, 13.56 mmol) and 4,7-dibromo-[1,2,5]thiadiazolo[3,4-*c*]pyridine (1.01 g, 3.42 mmol) in dry DMF (20 mL) was added $Pd(PPh_3)_4$ (0.38 g, 0.33 mmol), and the mixture was stirred at 95 °C under a nitrogen atmosphere until all the starting materials were consumed. After being cooled to room temperature, the mixture was poured into saturated aqueous brine, and then, the mixture was extracted with dichloromethane (3 × 20 mL). The crude product was washed twice with water, dried over anhydrous $MgSO_4$, and purified by silica column chromatography to afford 1.02 g of red solid (Yield: 71%). ^1H NMR (400 MHz, DMSO-d_6, ppm): δ 9.23 (s, 1H), 7.05 (s, 1H), 6.93 (s, 1H), 4.46 (s, 2H), 4.38 (s, 2H), 4.32 (s, 4H). ^{13}C NMR (400 MHz, DMSO-d_6, ppm): δ 154.37, 148.26, 142.28, 141.82, 141.68, 140.81, 125.75, 118.77, 111.24, 106.43, 102.86, 102.04, 65.52, 65.03, 64.41, 64.33. FT-IR (cm^{-1}): 3088, 2876, 1528, 1481, 1368, 1188, 1159, 1069, 999, 918, 874, 727, 631.

Electrochemical Experiments. Electrochemical experiments were carried out in a self-assembly electrolytic cell and controlled by a Model 263A potentiostat-galvanostat (EG&G Princeton Applied Research). The electrolytic cell contains two Pt wires and an Ag/AgCl electrode regarded as the working and counter electrodes and reference electrode, respectively. Besides, the solvent-electrolyte systems were blanked by nitrogen stream before each experiment.

The HOMO−LUMO levels and E_g values of EPTE and corresponding polymer are evaluated according to the empirical formulas as follows:[15,32]

$$\mathrm{HOMO} = -(E_{ox} + 4.80)\mathrm{eV} \quad (1)$$

$$\mathrm{LUMO} = (\mathrm{HOMO} + E_{g,opt})\mathrm{eV} \quad (2)$$

where E_{ox} and $E_{g,opt}$ are the onset oxidation potential and optical bandgap, respectively.

Electrochromic Tests. With a Cary 5000 spectrophotometer, spectroelectrochemistry and kinetic performances were determined in a self-assembly electrolytic cell, and the electrical conditions were controlled using a CHI 660D electrochemical workstation (Shanghai, China). The electrolytic cell consists of a transparent cuvette used as the container and an ITO-coated glass as the working electrode. The other devices are consistent with those used in the electrochemical experiment. All spectroelectrochemical and kinetic experiments were performed in MeCN−Bu_4NPF_6 (0.1 mol L^{-1}).

The optical density (ΔOD) and the coloration efficiency (CE) are calculated according to the following formulas:[1,37]

$$\Delta\mathrm{OD} = \log(T_{ox}/T_{red}) \quad (3)$$

$$\mathrm{CE} = \Delta\mathrm{OD}/Q_d \quad (4)$$

where T_{ox} and T_{red} are transmittance of oxidized and reduced polymer films, respectively. Q_d is injected/ejected charge per unit.

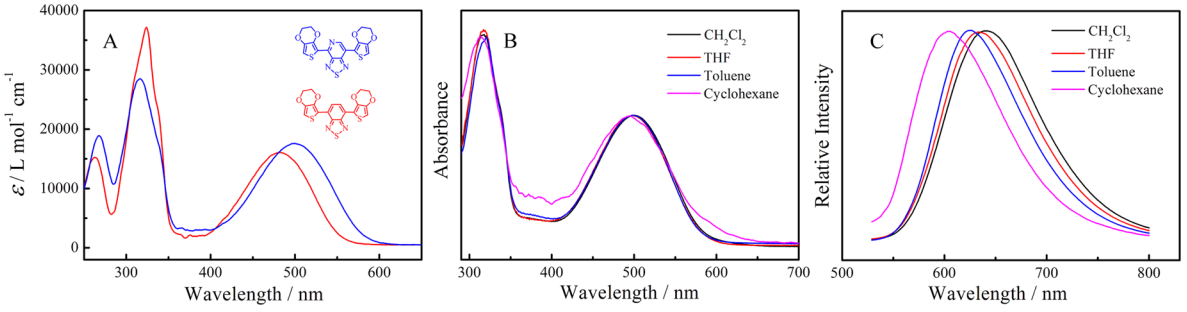

Figure 1. (A) Absorption spectra of EPTE and EBTE in CH_2Cl_2. (B) Absorption spectra of EPTE in cyclohexane, toluene, CH_2Cl_2, and THF. (C) Emission spectra of EPTE in cyclohexane, toluene, CH_2Cl_2, and THF.

DOI: 10.1021/acsami.5b01188
ACS Appl. Mater. Interfaces 2015, 7, 11089−11098

Table 1. Calculated and Experimental Data for EPTE, EBTE, and Their Polymers[a]

sample	$\lambda_{max,1}$ (nm)	$\lambda_{max,2}$ (nm)	$\lambda_{max,3}$ (nm)	H^{exp}/H^{DFT} (eV)	L^{exp}/L^{DFT} (eV)	$E_{g,ele}$ (eV)	$E_{g,opt}$ (eV)	$E_{g,DFT}$ (eV)
EPTE	266	315	500	−5.69/−5.03	−3.55/−2.56	–	2.14	2.47
PEPTE	427	756	–	−4.77/–	−3.65/–	0.85	1.12	–
EBTE	262	321	481	−5.50/−4.90	−3.25/−2.29	–	2.25	2.61
PEBTE	428	755	–	−4.65/–	−3.46/–	1.07	1.19	–

[a] H^{exp} and L^{exp} are the HOMO and LUMO levels estimated by empirical formulas, respectively. H^{DFT} and L^{DFT} are the HOMO and LUMO levels acquired through density functional theory calculations.

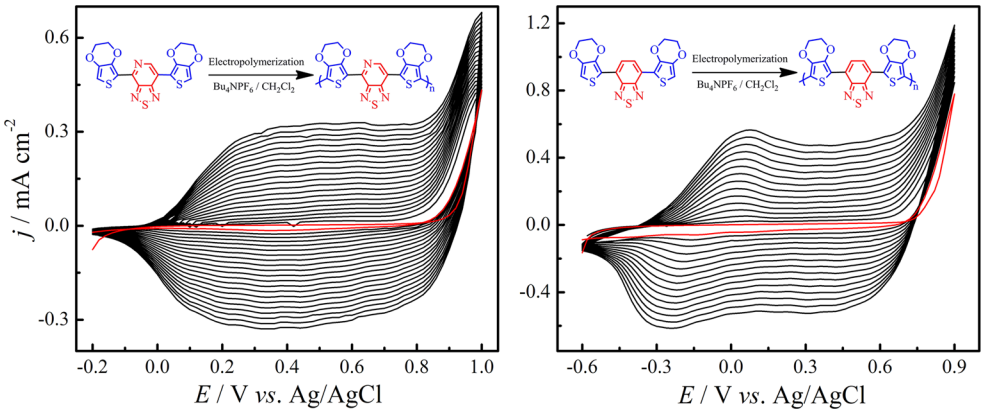

Figure 2. Cyclic voltammograms (CVs) of EPTE and EBTE in CH_2Cl_2−Bu_4NPF_6 (0.1 mol L^{-1}) at the potential scan rate of 100 mV s^{-1}. Monomer concentration: 5 mmol L^{-1}.

3. RESULTS AND DISCUSSION

Synthesis. First, the synthetic strategy (Scheme 2) to EPTE requires a π-electron deficient acceptor unit (III) as the building block. Starting from 3,4-diaminopyridine, compound II was synthesized according to previously reported procedures.[32] To achieve compound III with high yield, the conversion of compound II to the resulting compound III was conducted through a ring closure reaction in the presence of thionyl bromide instead of thionyl chloride. From the π-electron deficient dibromoheteroarene building block, EPTE was synthesized through Stille coupling reaction with a satisfactory yield (71%). ^{1}H and ^{13}C NMR spectra of EPTE were exhibited in the Supporting Information. For ease of comparison studies, EBTE was synthesized as previously described (Scheme S1, Supporting Information).[42]

Optical Property. To obtain the structure−property interrelation of D−A monomers, the optical properties of EPTE and EBTE were investigated initially. Both of the monomers showed dual-band absorption spectra, which was a distinguishing signature generally observed in donor−acceptor-type monomers.[43−46] Also, EBTE and EPTE spectra were so close due to a similar structure. The high-energy absorption band (280−360 nm) originated from π−π^* transition of EDOT, while the low-energy absorption band was owing to the charge transfer from EDOT to PT. In addition, the low-energy absorption band of EPTE was blue-shifted about 6 nm as compared with EBTE (Figure 1A and Table 1). This behavior could be attributed to the higher electronegativity of N that changed the ionization potential of the donor−acceptor-type system.[42,43] In addition, by comparison with EBTE, the low-energy band of EPTE shifted to longer wavelength with increasing absorption coefficient, which may be due to the π-electron deficient nature of pyridine ring compared to benzene since it was easier to transfer charge from the donor to acceptor units (Figure 1A, Tables 1 and S2, Supporting Information).[45,46] To confirm this behavior, the solvatochromic experiments have been performed. It was expected that the polar excited state of D−A monomer was more stable than the less polar ground state of D−A monomer in more polar solvent. Therefore, the emission spectra the monomer should shift to a longer wavelength in more polar solvents.

Specifically, absorption and emission spectra were tested in solvents with increasing dielectric constants: cyclohexane (ε = 2.0), toluene (ε = 2.4), THF (ε = 7.5), and CH_2Cl_2 (ε = 8.9). The absorption spectra of EPTE appeared constant by changing the polarity of solvent, with low-energy absorption peak at approximately 500 nm (Figure 1B). As expected, the emission spectra of EPTE exhibited redshift in more polar solvents (Figure 1C and Table S3, Supporting Information). This redshift with increasing the polarity of solvent confirmed the explanation mentioned earlier.

Electrochemical Polymerization. The electropolymerization performances of monomers were examined in the CH_2Cl_2−Bu_4NPF_6 (0.1 mol L^{-1}) system. The onset oxidation potential ($E_{ox,m}$) of EPTE (0.89 V, Figure S1, Supporting Information) was found to be higher than that of EBTE (0.70 V). The difference further confirmed that PT-based donor−acceptor systems were more electron deficient compared to BT-based systems.[7]

As depicted in Figure 2, the occurrence of the current loop beyond E_{onset} was the sign of the nucleation of EPTE and EBTE.[47] During the potentiodynamic electropolymerization, the progressive increase of the currents demonstrated that the electroactive polymers were formed.[48−50] From the CV results, both poly(4,7-di(2,3-dihydrothieno[3,4-*b*][1,4]dioxin-5-yl)-[1,2,5] thiadiazolo[3,4-*c*]pyridine) (PEPTE) and poly(4,7-di(2,3-dihydrothieno[3,4-*b*][1,4]dioxin-5-yl)benzo[1,2,5]-thiadiazole) (PEBTE) exhibited broad redox waves. It is a commonly observed phenomenon for EDOT-based compounds during the electropolymerization and might be attributed to (1) the formation of conjugated polymer with

DOI: 10.1021/acsami.5b01188
ACS Appl. Mater. Interfaces 2015, 7, 11089−11098

different chain length and (2) the mutual transition of multiple conductive species during the electropolymerization.[49−52] However, note here that the redox peak current densities for PEPTE film (0.24 mA cm^{-2}, 15 cycles of CVs) were much lower than those of PEBTE (0.57 mA cm^{-2}, 15 cycles of CVs), which may be explained by relatively higher electrical conductivity of the electrodeposited PEBTE.[48,53]

Optimization of Electrical Conditions. The performance and the quality of electropolymerized polymer are interrelated. Therefore, choosing the optimized potential for polymerization is essential toward high quality polymer film. A series of applied potentials were explored (EPTE: from 0.85 to 1.25 V; EBTE: from 0.70 to 1.00 V) during the electropolymerization of EPTE and EBTE, as shown in Figure S2, Supporting Information. As for the low applied potentials employed for the electropolymerization tests, they are due to the fact that the onset oxidation potentials of monomers during electrochemical tests usually change/drift due to influences of many factors, such as scan rates, reference electrodes, etc. Typically, there was no sign that PEPTE/PEBTE adhered on the electrode surface at potentials below $E_{ox,m}$. Also, the applied potentials beyond $E_{ox,m}$ led to the formation of polymers. By visual inspection during the experiments and chronoamperograms in Figure S2, Supporting Information, incorporating with these elements, and connecting with the quality of the polymer, the optimized applied potentials of EPTE and EBTE were 1.0 and 0.85 V, respectively. As expected, the optimized polymerization potential of EBTE was lower than EPTE, which was mainly due to different electron-deficient ability of acceptor units.[7] Therefore, all the polymers for electrochemical and electrochromic experiments were polymerized at the optimized potentials.

Structural Characterization. Considering the mechanism of electropolymerization, the polymerization of EPTE would only happen at the thiophene or pyridine ring. Compared with thiophene rings, the pyridine ring is electron deficient; thus, it is very difficult to eletropolymerize.[26,30] Also, significant steric hindrance would further impede the occurrence of eletropolymerization on the pyridine ring. Therefore, the electropolymerization would only happen at thiophene rings.

For the insoluble polymers, the vibrational spectrum is an expedient method to explore the polymerization mechanism. Hence, FT-IR spectra of EPTE and PEPTE were measured (Figure S3, Supporting Information), and FT-IR spectral peak assignment for EPTE and doped PEPTE was listed in Table S4, Supporting Information. In the functional group region, the peak at 3088 cm^{-1} in the FT-IR spectrum of EPTE is attributed to the =C−H vibration of the EDOT; however, the peak disappeared in the spectrum of PEPTE. The phenomenon indicated that EPTE could be electropolymerized at α-position of EDOT. In the fingerprint region, the peak at 1188 cm^{-1} should be assigned to the =C−H in-plane deformation vibration of EDOT, and 874 cm^{-1} results from out-of-plane deformation vibration. However, all these peaks disappear/weaken in FT-IR spectrum of the polymer, which further demonstrated that EPTE is electropolymerized through α,α'-coupling of EDOT units. For PEPTE, the peaks at 1485 and 1433 cm^{-1} could be attributed to the C=C skeletal vibration of EDOT, while the 1358 and 1302 and 1066 cm^{-1} result from the stretching of single C−C bond and the C−O vibration, respectively. For the pyridine group, these absorption peaks originating from the ring vibration can be observed at 1587 and 1551 cm^{-1}. The obvious absorption peak at 840 cm^{-1} should be the results of doping of PF_6^- ions into the polymer.

Density Functional Theory Calculations. To obtain a further interpretation of monomers, including planar structure, HOMO−LUMO levels, and bandgap, density functional theory calculations have been performed (Table 1 and Figure 3). A

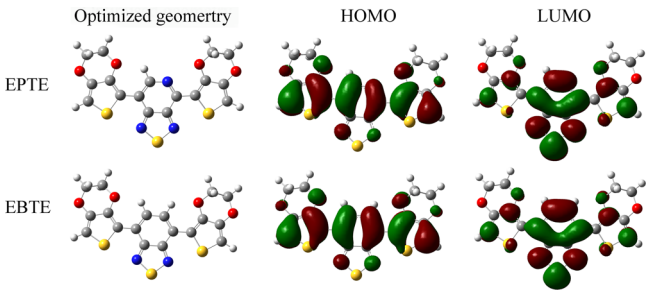

Figure 3. Optimized structures and HOMO−LUMO levels of EPTE and EBTE.

previous study demonstrated that HOMO−LUMO positions resided largely on the donor and acceptor units, respectively. The LUMO of EPTE (−2.56 eV) was lower as compared to that of EBTE (−2.29 eV). However, the HOMO also showed a slight decrease from EBTE to EPTE.[24,28] In the D−A conjugated compound system, it is a commonly observed phenomenon that the LUMO position depends mainly on the acceptor unit. Also, these values were found to be higher than those from experimental data, which could be explained by solvent effect.

Electrochemistry of PEPTE. For a comparative study, the electrochemical behaviors of both PEPTE and PEBTE films were carried out in monomer-free MeCN−Bu_4NPF_6 and other electrolytes, as shown in Figures 4 and S4 and S5, Supporting Information. Similar to other EDOT-based electrochromic polymers, both PEPTE and PEBTE exhibited good redox activity in the MeCN−Bu_4NPF_6 system. However, PEBTE displayed well-defined n-doping/dedoping and p-doping/dedoping behaviors, while the n-doping/dedoping process for PEPTE was unsatisfactory (Figure S6, Supporting Information). Also, the electrochemical performance of PEPTE was explored in other solvent-electrolyte systems including CH_2Cl_2−Bu_4NPF_6, MeCN−Bu_4NBF_4, and MeCN−$LiClO_4$. Clearly, PEPTE revealed good redox activity and stability in all these media, but the electrochemical behaviors were slightly affected by solvent-electrolyte systems, such as redox potential range, redox peaks, current densities, the shape of CV curves, etc.

In these systems, it was exhibited that the scan rates were linear with the peak current densities (Figure 4). The linear dependency certified that PEPTE was closely attached to the Pt electrode and the electrochemical behaviors were nondiffusion determined.[48,50] Furthermore, the calculated $j_{p,a}/j_{p,c}$ values ($j_{p,a}$ or $j_{p,c}$ is calculated as the ratio between anodic or cathodic peak current density and potential scan rate) of PEPTE in MeCN−Bu_4NBF_4 and MeCN−$LiClO_4$ are closer to 1.0, better than those of PEPTE in CH_2Cl_2−Bu_4NPF_6 and MeCN−Bu_4NPF_6, demonstrating superior redox reversibility of PEPTE in MeCN−Bu_4NBF_4 and MeCN−$LiClO_4$. It was also found that the discrepancy in the redox peak potentials of PEPTE was obvious. This potential discrepancy could be attributed to several reasons: (1) slow transition of multiple conductive

DOI: 10.1021/acsami.5b01188
ACS Appl. Mater. Interfaces 2015, 7, 11089−11098

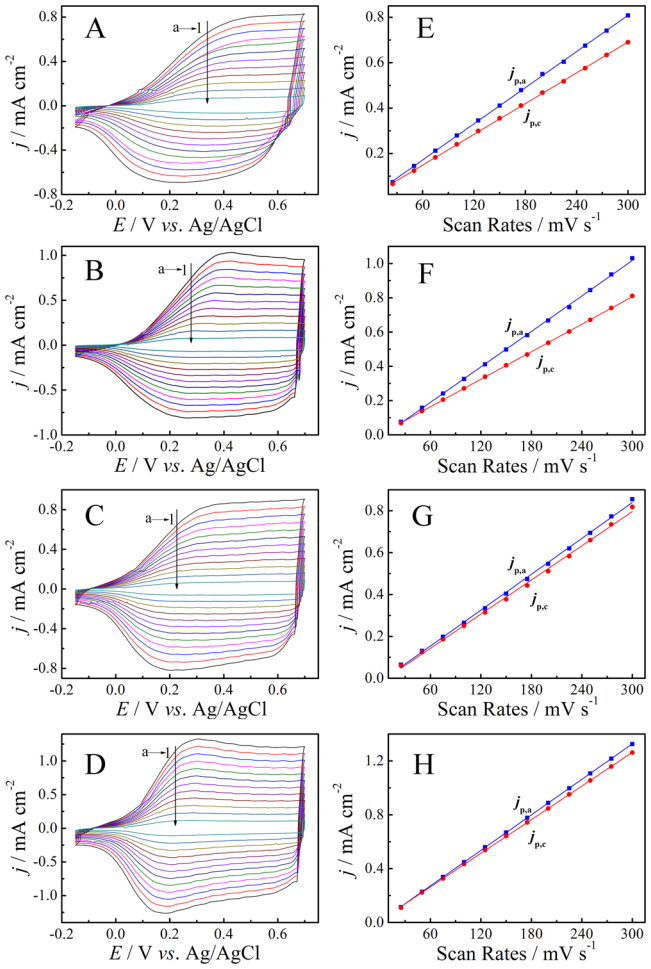

Figure 4. CVs of PEPTE in different solvent-electrolyte systems: (A) CH_2Cl_2–Bu_4NPF_6, (B) MeCN–Bu_4NPF_6, (C) MeCN–Bu_4NBF_4, and (D) MeCN–$LiClO_4$. Potential scan rates: 300–25 mV s^{-1}. Electrolyte concentrations: 0.1 mol L^{-1}. Left column: plots of redox peak current densities vs. potential scan rates for different solvent-electrolyte systems: (E) CH_2Cl_2–Bu_4NPF_6, (F) MeCN–Bu_4NPF_6, (G) MeCN–Bu_4NBF_4, and (H) MeCN–$LiClO_4$. j_p is the peak current density, and $j_{p,a}$ and $j_{p,c}$ denote the anodic and cathodic peak current densities, respectively.

species during the doping/dedoping process of PEPTE, (2) local rearrangement effect of conjugated polymer with different chain length, and (3) slow electron mobility at the interfaces including the solution/polymer and the polymer/electrode.[50,54]

The redox stability of PEPTE was systematically explored in different solvent-electrolyte systems (Figure 5). On the basis of exchange charge, the redox activities of PEPTE remain at 90%, 91%, and 70% after 2000 cycles in MeCN–Bu_4NPF_6, MeCN–Bu_4NBF_4, and MeCN–$LiClO_4$, respectively. Whereas in CH_2Cl_2–Bu_4NPF_6, its electrochemical activity maintained only 60% of the exchange charge retained after 600 cycles. The dissolution of active material from the working electrode contributed to the decrease in electrochemical activity of PEPTE, which could be certified through UV–vis spectra of the solvent-electrolyte systems finishing CV scanning (Figure S7, Supporting Information). The relatively poorer stability in CH_2Cl_2–Bu_4NPF_6 was mainly due to the better solubility of CH_2Cl_2 than MeCN for PEPTE films, causing a few oligomers with longer chain length to be dissolved from the electrode (Figure S7, Supporting Information).

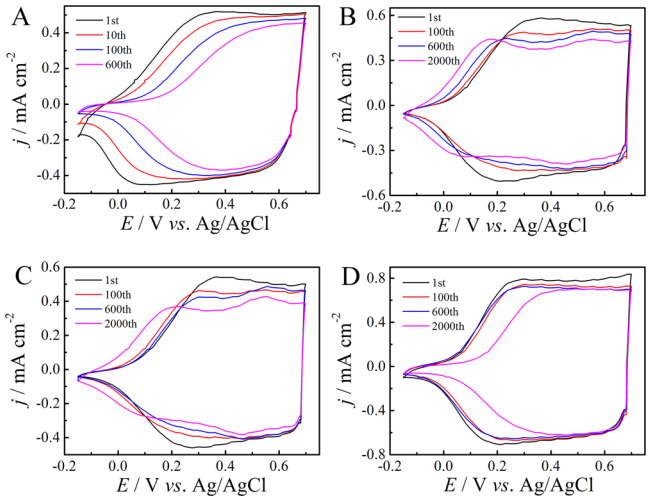

Figure 5. CVs of PEPTE in (A) CH_2Cl_2–Bu_4NPF_6, (B) MeCN–Bu_4NPF_6, (C) MeCN–Bu_4NBF_4, and (D) MeCN–$LiClO_4$ at the scan rate of 150 mV s^{-1}. Electrolyte concentrations: 0.1 mol L^{-1}.

Morphology. For analyzing the surface morphology, constituent, and texture of PEPTE and PEBTE, scanning electron microscopy (SEM) has been performed (Figure 6). Clearly, both PEPTE and PEBTE films showed homogeneous and smooth surface morphology macroscopically and even at the magnification of 2000× due to their similar chemical structures. At high magnifications (50 000×), both of the polymer films still resembled compact and ordered arrangements of globules. This is a common morphology often observed for electrosynthesized conducting polymer films and also in good agreement with those of previous reports. Note here that the surface of PEPTE seems a little smoother and denser than PEBTE.[16] In terms of morphology, the doped polymer films exhibited no obvious difference compared to the dedoped polymer films, indicating that the immigration/emigration of counterions in doping/dedoping processes did not destroy their original surface of polymer films.

Spectroelectrochemistry. The spectroelectrochemistry of PEPTE upon oxidation was performed to elucidate the electronic properties, as shown in Figure 7A. As expected, PEPTE exhibited a duel-band absorption spectrum in the neutral state located in 427 and 756 nm, which was indispensable to achieve neutral green electrochromic polymer.[1,4] The low-energy absorption peak of PEPTE shifted to a longer wavelength of about 2 nm as compared with PEBTE, while the absorption peak of corresponding monomer was red-shifted about 20 nm. The result could be due to the lower chain length relative to PEBTE changing the conjugation effect. Upon oxidation of PEPTE, the intensities of the two bands decreased simultaneously, and an obvious absorption of the polaron started to intensify in the near-infrared region. At the same time, the color of PEPTE changed from green (L: 56.00, a: −25.75, b: 11.45) to blue (L: 54.67, a: −24.16, b: −16.17). It is noteworthy to mention that the absorption band at longer wavelength almost coincided with the new polaronic absorption band. For the achievement of transmissive polymer in the oxidized state, future work may be focused on changing (1) the low-energy absorption region by exchange of the donor or acceptor unit and (2) the polaronic absorption band through the use of electrolyte variations.[36]

DOI: 10.1021/acsami.5b01188
ACS Appl. Mater. Interfaces 2015, 7, 11089–11098

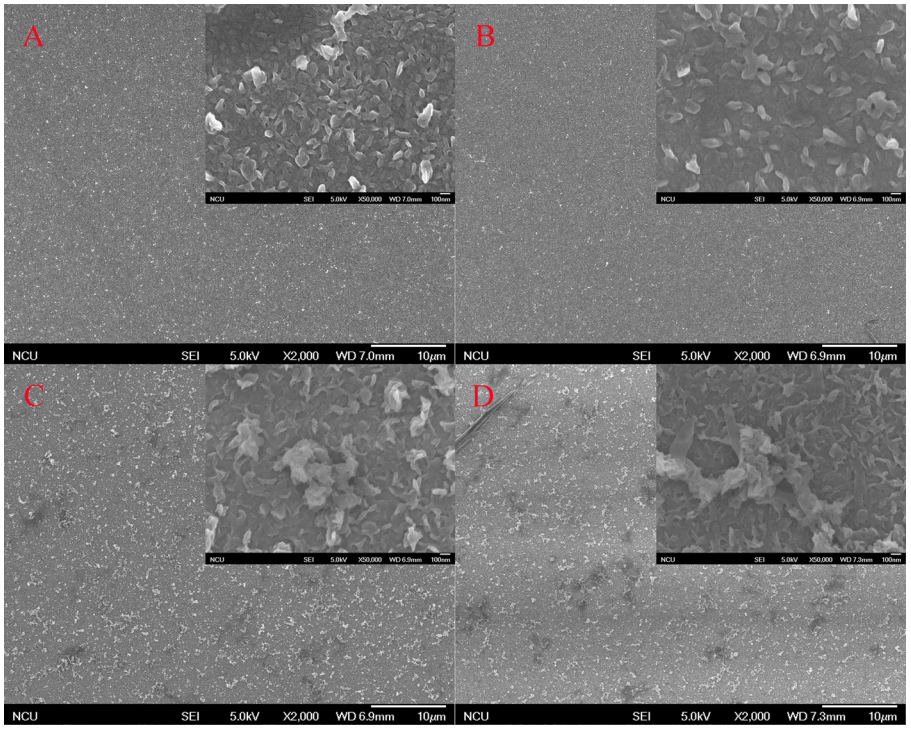

Figure 6. SEM images of doped PEPTE (A), dedoped PEPTE (B), doped PEBTE (C), and dedoped PEBTE (D) polymerized electrochemically on the ITO-coated glass. Magnification: 2000× and 50 000× (inset).

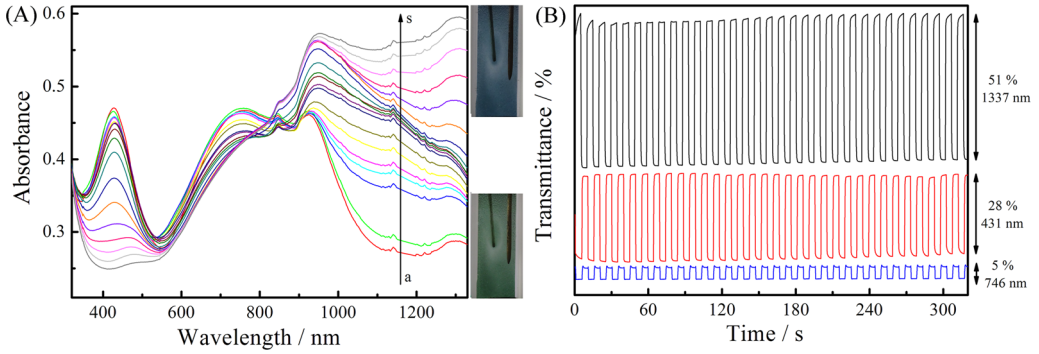

Figure 7. (A) Spectroelectrochemistry and switching colors of PEPTE film on an ITO-coated glass in MeCN–Bu_4NPF_6 (0.1 mol L^{-1}) at applied potentials of (a) −1.1 V, (b) −1.0 V, (c) −0.9 V, (d) −0.8 V, (e) −0.7 V, (f) −0.6 V, (g) −0.5 V, (h) −0.3 V, (i) −0.2 V, (j) 0 V, (k) 0.1 V, (l) 0.3 V, (m) 0.4 V, (n) 0.5 V, (o) 0.6 V, (p) 0.7 V, (q) 0.8 V, (r) 0.9 V, and (s) 1.1 V. (B) Transmittance change during the electrochromic switching of PEPTE in MeCN–Bu_4NPF_6 (0.1 mol L^{-1}). Switching time: 5 s.

Table 2. Electrochromic Parameters for PEPTE and PEBTE

					response time (s)		
sample	wavelength (nm)	T_{red}, %	T_{ox}, %	ΔT, %	oxidation	reduction	CE (cm^2 C^{-1})
PEPTE	431	20	48	28	1.0	0.3	154
	746	13	18	5	0.6	0.3	109
	1337	69	18	51	0.6	0.3	257
PEBTE[a]	428	43	80	37		<1.0	130
	755	–	–	23		0.4	–
	1500	–	–	72		1.0	–
PEBTE[b]	428	43	8	37	1.8	1.0	86
	755	26	49	23	0.6	0.8	52
	1100	81	43	38	1.0	2.2	109

[a]Previous results from ref 16 by Toppare and co-workers. Unreported data are shown with a dashed line. [b]Our experimental results.

Also, the bandgap of PEPTE (1.12 eV), calculated from the second absorption, was a little higher than that obtained from the electrochemical experimental result (0.85 eV) (Table 1, Figures 7A and S8, Supporting Information). Generally,

DOI: 10.1021/acsami.5b01188
ACS Appl. Mater. Interfaces 2015, 7, 11089−11098

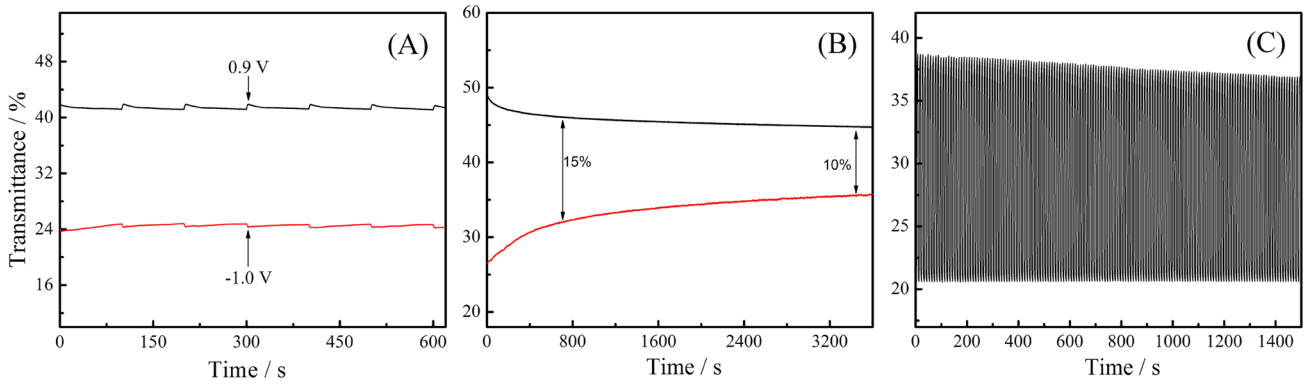

Figure 8. Open circuit memory of PEPTE monitored at 431 nm MeCN−Bu_4NPF_6 (0.1 mol L^{-1}). (A) The potential was applied on PEPTE for 2 s, and then, PEPTE was potential-free for 100 s. (B) Long-term optical memory. (C) Optical stability at 431 nm between −0.15 and 0.70 V.

electronic bandgaps of conjugated polymers were higher than optical bandgaps due to residual charge. However, a similar observation has been reported for some D−A polymers (Table S1, Supporting Information).[16,17,24] The phenomenon might have originated from (1) photoinduced charge transfer from EDOT to PT in the D−A conjugated system[23] and (2) the interfacial resistance involving the polymer/electrode.[55] In addition, the bandgap of PEPTE calculated from both CV curves and absorption spectra was relatively lower compared to PEBTE ($E_{g,ele}$ = 1.07 eV, $E_{g,opt}$ = 1.19 eV, Figure S9, Supporting Information). Being a stronger electron acceptor, the PT moiety not only modulates absorption characteristics of a conjugated polymer but also allows for tuning bandgap to a low value. As shown in Table 1, LUMO and HOMO of PEPTE, obtained from the experimental result, were observed to be lower than that of PEBTE. In addition, the decrease of LUMO was found to be higher than that of HOMO, which can be explained by the increasing electron-accepting ability of PT as in the case of monomer.

Electrochromic Properties. The electrochromic performance was explored by the double step chronoamperometry method (resident time: 5 s), and the transmittance curves between neutral and oxidized states were recorded. The electrochromic parameters for PEPTE and PEBTE, including transmittance change (ΔT), coloration efficiency (CE), response time, optical memory, and optical stability, were analyzed comparatively, and the electrochromic parameters of both PEPTE and PEBTE are summarized in Table 2.

PEPTE showed 28% optical contrast in the visible region (431 nm), whereas the optical contrasts at the donor−acceptor charge transfer band (746 nm) and NIR band (1337 nm) were 5% and 51%, respectively (Figure 7B). These values are higher than some analogous green electrochromic polymers (Scheme S1, Supporting Information) but apparently inferior to those of PEBTE (428 nm: 37%; 755 nm: 23%; 1500 nm: 72% by Toppare and co-workers;[16] 428 nm: 37%; 755 nm: 23%; 1100 nm: 38% by our results). The lower optical contrasts, especially at 746 nm, were probably ascribed to the absorption overlap between the low-energy band and the new polaronic absorption band.[24] Despite these values seeming to be a little lower than PEBTE, it was quite enough to get the green electrochromic polymer. In addition, PEPTE had a good ΔT of 51% at 1337 nm, which was a valuable character in near-infrared electrochromic materials.

Interestingly, PEPTE exhibited fast switching time between neutral and oxidized state and achieved 95% of the optical contrasts within 1 s at all three wavelengths (Table 2), especially in the reduction process (0.3 s at all three wavelengths). The switching of PEPTE was obviously faster than its close analog PEBTE (0.4−1.0 s at all wavelengths by Toppare and co-workers;[16] 0.6−2.2 s at all wavelengths by our repeated results under the same conditions). To the best of our knowledge, PEPTE exhibited the fastest switching time in these reported neutral state green electrochromic polymers (their typical response times in the range of 0.4−2.1 s),[13−27,33−36] which indicated the ease of diffusion of these counterbalancing ions across PEPTE.[23]

Coloration efficiency (CE) is regarded as a valuable standard for judging the electrochromic performance and obtained from eqs 3 and 4. For PEPTE, CE was calculated to be 154 cm^2 C^{-1} at 431 nm and 109 cm^2 C^{-1} at 746 nm, respectively, clearly higher than PEBTE at similar wavelengths (130 cm^2 C^{-1} at 428 nm and 52 cm^2 C^{-1} at 755 nm). Moreover, the CE of PEPTE at 1337 nm was found to be as high as 257 cm^2 C^{-1}, whereas only 109 cm^2 C^{-1} at 1100 nm was obtained for PEBTE.

The optical memory of electrochromic polymers is described as the ability to keep neutral/oxidized color without using the applied potential, which is closely associated with their applications, and the optical memory can be estimated by the transmittance curve. Initially, the potential of +0.9 V was applied on PEPTE film for 2 s, and then, PEPTE film was potential-free for 100 s. Simultaneously, the transmittance of oxidized PEPTE was measured. The same procedure was repeated with −1.0 V. As shown in Figures 8 and S11, Supporting Information, the color of the neutral/oxidized PEPTE was unchanged in the absence of applied potential. PEBTE showed stronger fluctuations (0.8 V: 5.3%; −0.8 V: 1.4%) in comparison with PEPTE (0.9 V: 0.7%; −1.0 V: 0.7%), which demonstrated PEPTE could minimize the self-erasing effect (electrochromic polymers freely diffuse and exchange electrons in the absence of applied voltage).[1]

The long-term optical memory is specially important for the application in electronic devices.[1,50] As shown in Figures 8 and S11, Supporting Information, the transmittance of neutral/oxidized PEPTE films was measured in the absence of applied voltage. The transmittance change of PEPTE between the neutral and oxidized state initially experienced a sharp decrease and finally kept almost constant at about 10%. A similar phenomenon can be observed for PEBTE film but with a sharper decrease in transmittance contrast and finally kept constant at about 15%.

DOI: 10.1021/acsami.5b01188
ACS Appl. Mater. Interfaces 2015, 7, 11089−11098

In addition, the degraded optical activity of PEPTE obtained after 100 cycles of operation was found to be 93% of the starting activity (Figure 8C), in agreement with CV results. By all accounts, PEPTE exhibited a typical electrochromic nature from neutral green to blue in the oxidized state with relatively high contrast ratios, good color persistence, and favorable stability. Furthermore, in comparison with its close analog PEBTE, PEPTE showed faster response time and higher CE values.

4. CONCLUSIONS

In conclusion, PT was regarded as a promising alternative to BT for D−A conjugated polymer and employed in electrochromic materials. The monomers (EPTE and EBTE) and the corresponding polymers (PEPTE and PEBTE) were comparatively investigated, including quantum chemistry calculations, structure characterization, surface morphology, and electrochemical, spectroelectrochemical, and electrochromic properties. Compared to PEBTE, PEPTE revealed higher efficiencies, favorable optical memory, lower bandgap (0.85 eV), and faster response time (0.3 s). From these preliminary results, PT is probably a promising choice for the design of excellent electrochromic polymers by matching with various donor units. The rational design of new D−A electrochromic materials containing PT derivatives toward high optical contrasts is under investigation in our laboratory.

■ ASSOCIATED CONTENT

Ⓢ Supporting Information

Synthesis procedure, FT-IR characterization, and additional electrochemical data. The Supporting Information is available free of charge on the ACS Publications website at DOI: 10.1021/acsami.5b01188.

■ AUTHOR INFORMATION

Corresponding Authors

*Tel: +86-791-88537967. Fax: +86-791-83823320. E-mail: xujingkun@tsinghua.org.cn.

*Tel: +86-791-88537967. Fax: +86-791-83823320. E-mail: lby1258@163.com.

Notes

The authors declare no competing financial interest.

■ ACKNOWLEDGMENTS

We acknowledge the National Natural Science Foundation of China (grant numbers: 51303073, 51463008), Ganpo Outstanding Talents 555 projects (2013), the Training Plan for the Main Subject of Academic Leaders of Jiangxi Province (2011), the Natural Science Foundation of Jiangxi Province (grant numbers: 20122BAB216011 and 20142BAB216029), the Science and Technology Landing Plan of Universities in Jiangxi Province (KJLD12081), Provincial Projects for Postgraduate Innovation in Jiangxi (YC2014-S441, YC2014-S431), and Scientific Research Projects of Jiangxi Science & Technology Normal University (2014QNBJRC003) for their financial support.

■ ABBREVIATIONS

PT, thiadiazolo[3,4-*c*]pyridine
BT, benzothiadiazole
EDOT, 3,4-ethylenedioxythiophene
EPTE, 4,7-di(2,3-dihydrothieno[3,4-*b*][1,4]dioxin-5-yl)-[1,2,5]thiadiazolo[3,4-*c*]pyridine
PEPTE, poly(4,7-di(2,3-dihydrothieno[3,4-*b*][1,4]dioxin-5-yl)-[1,2,5]thiadiazolo[3,4-*c*]pyridine)
EBTE, 4,7-di(2,3-dihydrothieno[3,4-*b*][1,4]dioxin-5-yl)-benzo[1,2,5]thiadiazole
PEBTE, poly(4,7-di(2,3-dihydrothieno[3,4-*b*][1,4]dioxin-5-yl)benzo[1,2,5]thiadiazole)

■ REFERENCES

(1) Beaujuge, P. M.; Reynolds, J. R. Color Control in π-Conjugated Organic Polymers for Use in Electrochromic Devices. *Chem. Rev.* **2010**, *110*, 268−320.
(2) Beaujuge, P. M.; Amb, C. M.; Reynolds, J. R. Spectral Engineering in π-Conjugated Polymers with Intramolecular Donor-Acceptor Interactions. *Acc. Chem. Res.* **2010**, *43*, 1396−1407.
(3) Groenendaal, L.; Zotti, G.; Aubert, P.; Waybright, S. M.; Reynolds, J. R. Electrochemistry of Poly(3,4-alkylenedioxythiophene) Derivatives. *Adv. Mater.* **2003**, *15*, 855−879.
(4) Gunbas, G.; Toppare, L. Electrochromic Conjugated Polyheterocycles and Derivatives-Highlights from the Last Decade towards Realization of Long Lived Aspirations. *Chem. Commun.* **2012**, *48*, 1083−1101.
(5) Amb, C. M.; Dyer, A. L.; Reynolds, J. R. Navigating the Color Palette of Solution-Processable Electrochromic Polymers. *Chem. Mater.* **2011**, *23*, 397−415.
(6) Dyer, A. L.; Craig, M. R.; Babiarz, J. E.; Kiyak, K.; Reynolds, J. R. Orange and Red to Transmissive Electrochromic Polymers Based on Electron-Rich Dioxythiophenes. *Macromolecules* **2010**, *43*, 4460−4467.
(7) Kerszulis, J. A.; Amb, C. M.; Dyer, A. L.; Reynolds, J. R. Follow the Yellow Brick Road: Structural Optimization of Vibrant Yellow-to-Transmissive Electrochromic Conjugated Polymers. *Macromolecules* **2014**, *47*, 5462−5469.
(8) Beaujuge, P. M.; Ellinger, S.; Reynolds, J. R. The Donor-Acceptor Approach Allows a Black-to-Transmissive Switching Polymeric Electrochrome. *Nat. Mater.* **2008**, *7*, 795−799.
(9) Steckler, T. T.; Henriksson, P.; Mollinger, S.; Lundin, A.; Salleo, A.; Andersson, M. R. Very Low Band Gap Thiadiazoloquinoxaline Donor-Acceptor Polymers as Multi-Tool Conjugated Polymers. *J. Am. Chem. Soc.* **2014**, *136*, 1190−1193.
(10) Wang, X.; Chen, Y.; Chen, X. Cooperative Non-Covalent Interaction for Organic Molecular Recognition and Self-Assembly. *Prog. Chem.* **2005**, *17*, 451−458.
(11) Kerszulis, J. A.; Johnson, K. E.; Kuepfert, M.; Khoshabo, D.; Dyer, A. L.; Reynolds, J. R. Tuning the Painter's Palette: Subtle Steric Effects on Spectra and Colour in Conjugated Electrochromic Polymers. *J. Mater. Chem. C* **2015**, *3*, 3211−3218.
(12) Beverina, L.; Pagani, G. A.; Sassi, M. Multichromophoric Electrochromic Polymers: Colour Tuning of Conjugated Polymers through the Side Chain Functionalization Approach. *Chem. Commun.* **2014**, *50*, 5413−5430.
(13) Sonmez, G.; Shen, C. K. F.; Rubin, Y.; Wudl, F. A Red, Green, and Blue (RGB) Polymeric Electrochromic Device (PECD): The Dawning of the PECD Era. *Angew. Chem.* **2004**, *116*, 1524−1528.
(14) Sonmez, G. Polymeric Electrochromics. *Chem. Commun.* **2005**, 5251−5259.
(15) İçli, M.; Pamuk, M.; Algi, F.; Önal, A. M.; Cihaner, A. Donor-Acceptor Polymer Electrochromes with Tunable Colors and Performance. *Chem. Mater.* **2010**, *22*, 4034−4044.
(16) Durmus, A.; Gunbas, G. E.; Camurlu, P.; Toppare, L. A Neutral State Green Polymer with a Superior Transmissive Light Blue Oxidized State. *Chem. Commun.* **2007**, 3246−3248.
(17) Algi, F.; Cihaner, A. An Ambipolar Neutral State Green Polymeric Electrochromic. *Org. Electron.* **2009**, *10*, 704−710.
(18) Beaujuge, P. M.; Ellinger, S.; Reynolds, J. R. Spray Processable Green to Highly Transmissive Electrochromics via Chemically Polymerizable Donor-Acceptor Heterocyclic Pentamers. *Adv. Mater.* **2008**, *20*, 2772−2776.

DOI: 10.1021/acsami.5b01188
ACS Appl. Mater. Interfaces 2015, 7, 11089−11098

(19) Durmus, A.; Gunbas, G. E.; Toppare, L. New, Highly Stable Electrochromic Polymers from 3,4-Ethylenedioxythiophene-Bis-Substituted Quinoxalines toward Green Polymeric Materials. *Chem. Mater.* **2007**, *19*, 6247−6251.
(20) Celebi, S.; Balan, A.; Epik, B.; Baran, D.; Toppare, L. Donor Acceptor Type Neutral State Green Polymer Bearing Pyrrole as the Donor Unit. *Org. Electron.* **2009**, *10*, 631−636.
(21) Özdemira, Ş.; Balana, A.; Barana, D.; Doğana, Ö.; Topparea, L. Green to Highly Transmissive Switching Multicolored Electrochromes: Ferrocene Pendant Group Effect on Electrochromic Properties. *React. Funct. Polym.* **2011**, *71*, 168−174.
(22) Tarkuc, S.; Udum, Y. A.; Toppare, L. Tuning of the Neutral State Color of the Conjugated Donor-Acceptor-Donor Type Polymer from Blue to Green via Changing the Donor Strength on the Polymer. *Polymer* **2009**, *50*, 3458−3464.
(23) Xu, Z.; Wang, M.; Zhao, J.; Cui, C.; Fan, W.; Liu, J. Donor-Acceptor Type Neutral Green Polymers Containing 2,3-Di(5-methylfuran-2-yl) Quinoxaline Acceptor and Different Thiophene Donors. *Electrochim. Acta* **2014**, *125*, 241−249.
(24) Cihaner, A.; Algi, F. A Novel Neutral State Green Polymeric Electrochromic with Superior n- and p-Doping Processes: Closer to Red-Blue-Green (RGB) Display Realization. *Adv. Funct. Mater.* **2008**, *18*, 3583−3589.
(25) Gunbas, G. E.; Durmus, A.; Toppare, L. Could Green be Greener? Novel Donor-Acceptor-Type Electrochromic Polymers: Towards Excellent Neutral Green Materials with Exceptional Transmissive Oxidized States for Completion of RGB Color Space. *Adv. Mater.* **2008**, *20*, 691−695.
(26) Gunbas, G. E.; Durmus, A.; Toppare, L. A Unique Processable Green Polymer with a Transmissive Oxidized State for Realization of Potential RGB-Based Electrochromic Device Applications. *Adv. Funct. Mater.* **2008**, *18*, 2026−2030.
(27) Nikolou, M.; Dyer, A. L.; Steckler, T. T.; Donoghue, E. P.; Wu, Z.; Heston, N. C.; Rinzler, A. G.; Tanner, D. B.; Reynolds, J. R. Dual *n*- and *p*-Type Dopable Electrochromic Devices Employing Transparent Carbon Nanotube Electrodes. *Chem. Mater.* **2009**, *21*, 5539−5547.
(28) Cheng, Y.-J.; Yang, S.-H.; Hsu, C.-S. Synthesis of Conjugated Polymers for Organic Solar Cell Applications. *Chem. Rev.* **2009**, *109*, 5868−5923.
(29) Zhou, H.; Yang, L.; Price, S. C.; Knight, K. J.; You, W. Enhanced Photovoltaic Performance of Low-Bandgap Polymers with Deep LUMO Levels. *Angew. Chem.* **2010**, *122*, 8164−8167.
(30) Blouin, N.; Michaud, A.; Gendron, D.; Wakim, S.; Blair, E.; Neagu-Plesu, R.; Belletête, M.; Durocher, G.; Tao, Y.; Leclerc, M. Toward a Rational Design of Poly(2,7-Carbazole) Derivatives for Solar Cells. *J. Am. Chem. Soc.* **2008**, *130*, 732−742.
(31) Liu, J.; Chen, Q. Advances in Synthesis and Application of Imidazopyridine Derivatives. *Prog. Chem.* **2010**, *22*, 631−638.
(32) Sun, Y.; Chien, S.-C.; Yip, H.-L.; Zhang, Y.; Chen, K.-S.; Zeigler, D. F.; Chen, F.-C.; Lin, B.; Jen, A. K. Y. High-Mobility Low-Bandgap Conjugated Copolymers Based on Indacenodithiophene and Thiadiazolo[3,4-*c*]pyridine Units for Thin Film Transistor and Photovoltaic Applications. *J. Mater. Chem.* **2011**, *21*, 13247−13255.
(33) Henson, Z. B.; Welch, G. C.; Poll, T.; Bazan, G. C. Pyridalthiadiazole-Based Narrow Band Gap Chromophores. *J. Am. Chem. Soc.* **2012**, *134*, 3766−3779.
(34) Sonmez, G.; Sonmez, H. B.; Shen, C. K. F.; Jost, R. W.; Rubin, Y.; Wudl, F. A Processable Green Polymeric Electrochromic. *Macromolecules* **2005**, *38*, 669−675.
(35) Hellström, S.; Cai, T.; Inganäs, O.; Andersson, M. R. Influence of Side Chains on Electrochromic Properties of Green Donor-Acceptor-Donor Polymers. *Electrochim. Acta* **2011**, *56*, 3454−3459.
(36) DuBois, C. J.; Abboud, K. A.; Reynolds, J. R. Electrolyte-Controlled Redox Conductivity and n-Type Doping in Poly(bis-EDOT-pyridine)s. *J. Phys. Chem. B* **2004**, *108*, 8550−8557.
(37) Qin, L.; Xu, J.; Lu, B.; Lu, Y.; Duan, X.; Nie, G. Synthesis and Electrochromic Properties of Polyacrylate Functionalized Poly(3,4-ethylenedioxythiophene) Network Films. *J. Mater. Chem.* **2012**, *22*, 18345−18353.
(38) Lu, B.; Zhen, S.; Zhang, S.; Xu, J.; Zhao, G. Highly Stable Hybrid Selenophene-3,4-Ethylenedioxythiophene as Electrically Conducting and Electrochromic Polymers. *Polym. Chem.* **2014**, *5*, 4896−4908.
(39) Wang, Z.; Xu, J.; Lu, B.; Zhang, S.; Qin, L.; Mo, D.; Zhen, S. Poly(thieno[3,4-*b*]-1,4-oxathiane): Medium Effect on Electropolymerization and Electrochromic Performance. *Langmuir* **2014**, *30*, 15581−15589.
(40) Zhen, S.; Xu, J.; Lu, B.; Zhang, S.; Zhao, L.; Li, J. Tuning the Optoelectronic Properties of Polyfuran by Design of Furan-EDOT Monomers and Free-standing Films with Enhanced Redox Stability and Electrochromic Performances. *Electrochim. Acta* **2014**, *146*, 666−678.
(41) Zhu, S. S.; Swager, T. M. Conducting Polymetallorotaxanes: Metal Ion Mediated Enhancements in Conductivity and Charge Localization. *J. Am. Chem. Soc.* **1997**, *119*, 12568−12577.
(42) Aldakov, D.; Palacios, M. A.; Anzenbacher, P. Benzothiadiazoles and Dipyrrolyl Quinoxalines with Extended Conjugated Chromophores-Fluorophores and Anion Sensors. *Chem. Mater.* **2005**, *17*, 5238−5241.
(43) Wang, E. G.; Li, C.; Zhuang, W. L.; Peng, J. B.; Cao, Y. High-Efficiency Red and Green Light-Emitting Polymers Based on a Novel Wide Bandgap Poly(2,7-silafluorene). *J. Mater. Chem.* **2008**, *18*, 797−801.
(44) Wang, E.; Wang, M.; Wang, L.; Duan, C.; Zhang, J.; Cai, W.; He, C.; Wu, H.; Cao, Y. Donor Polymers Containing Benzothiadiazole and Four Thiophene Rings in Their Repeating Units with Improved Photovoltaic Performance. *Macromolecules* **2009**, *42*, 4410−4415.
(45) Gibson, G. L.; McCormick, T. M.; Seferos, D. S. Atomistic Band Gap Engineering in Donor-Acceptor Polymers. *J. Am. Chem. Soc.* **2012**, *134*, 539−547.
(46) İçli-Özkut, M.; İpek, H.; Karabay, B.; Cihaner, A.; Önal, A. M. Furan and Benzochalcogenodiazole Based Multichromic Polymers via a Donor-Acceptor Approach. *Polym. Chem.* **2013**, *4*, 2457−2463.
(47) Skotheim, T. A. *Handbook of Conducting Polymer*; Marcel Dekker: New York, 1986.
(48) Skotheim, T. A.; Elsembaumer, R. L.; Reynolds, J. R. *Handbook of Conducting Polymer*, second ed.; Marcel Dekker: New York, 1998.
(49) Roncali, J. Conjugated Poiy(thiophenes): Synthesis, Functionalizatlon, and Applications. *Chem. Rev.* **1992**, *92*, 711−738.
(50) Chen, W.; Xue, G. Low Potential Electrochemical Syntheses of Heteroaromatic Conducting Polymers in a Novel Solvent System Based on Trifluroborate-Ethyl Ether. *Prog. Polym. Sci.* **2005**, *30*, 783−811.
(51) Shirakawa, H.; Louis, E. J.; Macdiarmid, A. G.; Macdiarmid, A. G.; Chiang, C. K.; Heeger, A. J. Synthesis of Electrically Conducting Organic Polymers: Halogen Derivatives of Polyacetylene $(CH)_n$. *J. Chem. Soc. Chem. Commun.* **1977**, 579−581.
(52) Elschner, A.; Kirchmeyer, S.; Lövenich, W.; Merker, U.; Reuter, K. *PEDOT: Principles and applications of an intrinsically conductive polymer*; CRC: Boca Raton, FL, 2011.
(53) Deng, S. X.; Advincula, R. C. Polymethacrylate Functionalized Polypyrrole Network Films on Indium Tin Oxide: Electropolymerization of a Precursor Polymer and Comonomer. *Chem. Mater.* **2002**, *14*, 4073−4080.
(54) Inzelt, G.; Pineri, M.; Schultze, J. W.; Vorotyntsev, M. A. Electron and Proton Conducting Polymers: Recent Developments and Prospects. *Electrochim. Acta* **2000**, *45*, 2403−2421.
(55) Egbe, D. A. M. L.; Nguyen, H.; Hoppe, H.; Muhlbacher, D.; Sariciftci, N. S. Side Chain Influence on Electrochemical and Photovoltaic Properties of Yne-Containing Poly(phenylenevinylene)s. *Macromol. Rapid Commun.* **2005**, *26*, 1389−1394.

DOI: 10.1021/acsami.5b01188
ACS Appl. Mater. Interfaces 2015, 7, 11089−11098